Supplementary Information

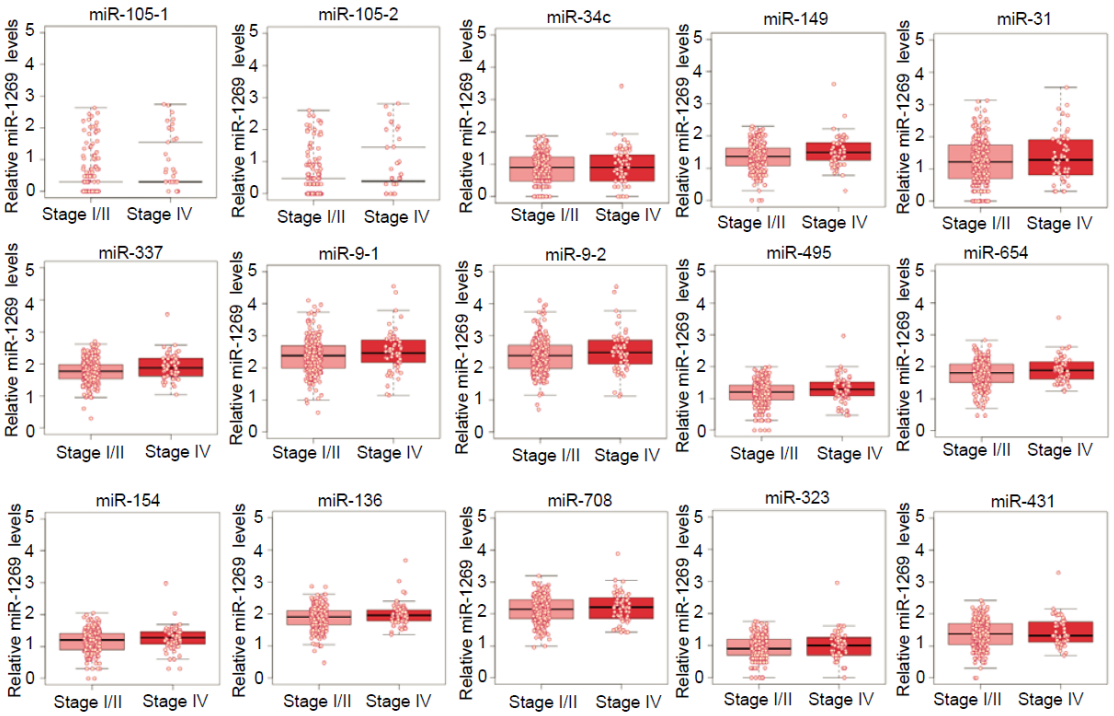

Supplementary Figure 1. microRNAs upregulated in late-stage CRCs according to TCGA. Expression levels of microRNAs from Table S1 in individual early- (stage I/II, n=230) and late-stage (stage IV, n=59) CRCs according to miRNASeq data from COAD.

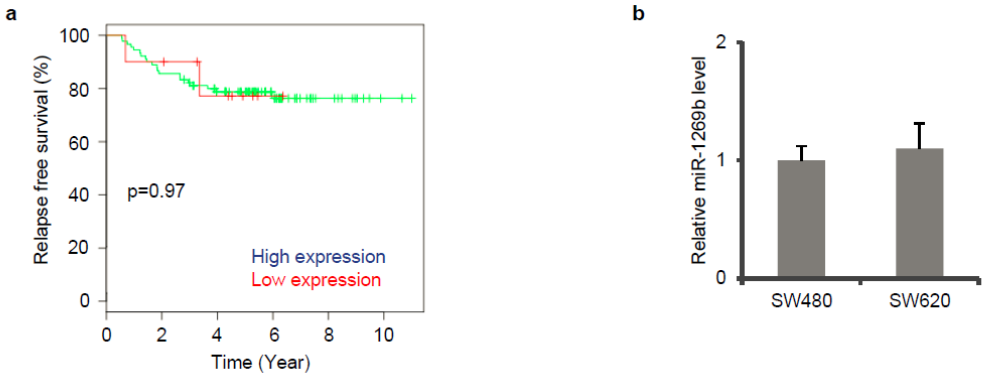

Supplementary Figure 2. miR-1269b is not associated with relapse.
(**a**) Kaplan-Meier analysis of relapses of Stage II CRC patients with high (red, n=10) and low (blue, n=90) miR-1269b levels in their surgically removed primary tumors. The p-value was calculated based on logrank test. (**b**) RT-qPCR of miR-1269b levels in SW480 and SW620 cells. Error bars denote s.d. of triplicates.

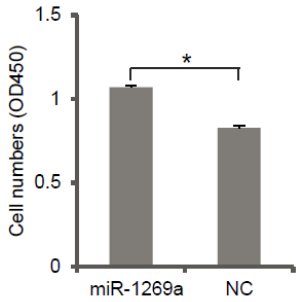

Supplementary Figure 3. The effect of miR-1269 on cell growth *in vitro*.
SWT-1 assay measuring the growth of SW480 cells with a control (NC) or a miR-1269a expression (miR-1269a) vector. Error bars denote the s.d. between triplicates. *, $p<0.05$, Student's *t*-test.

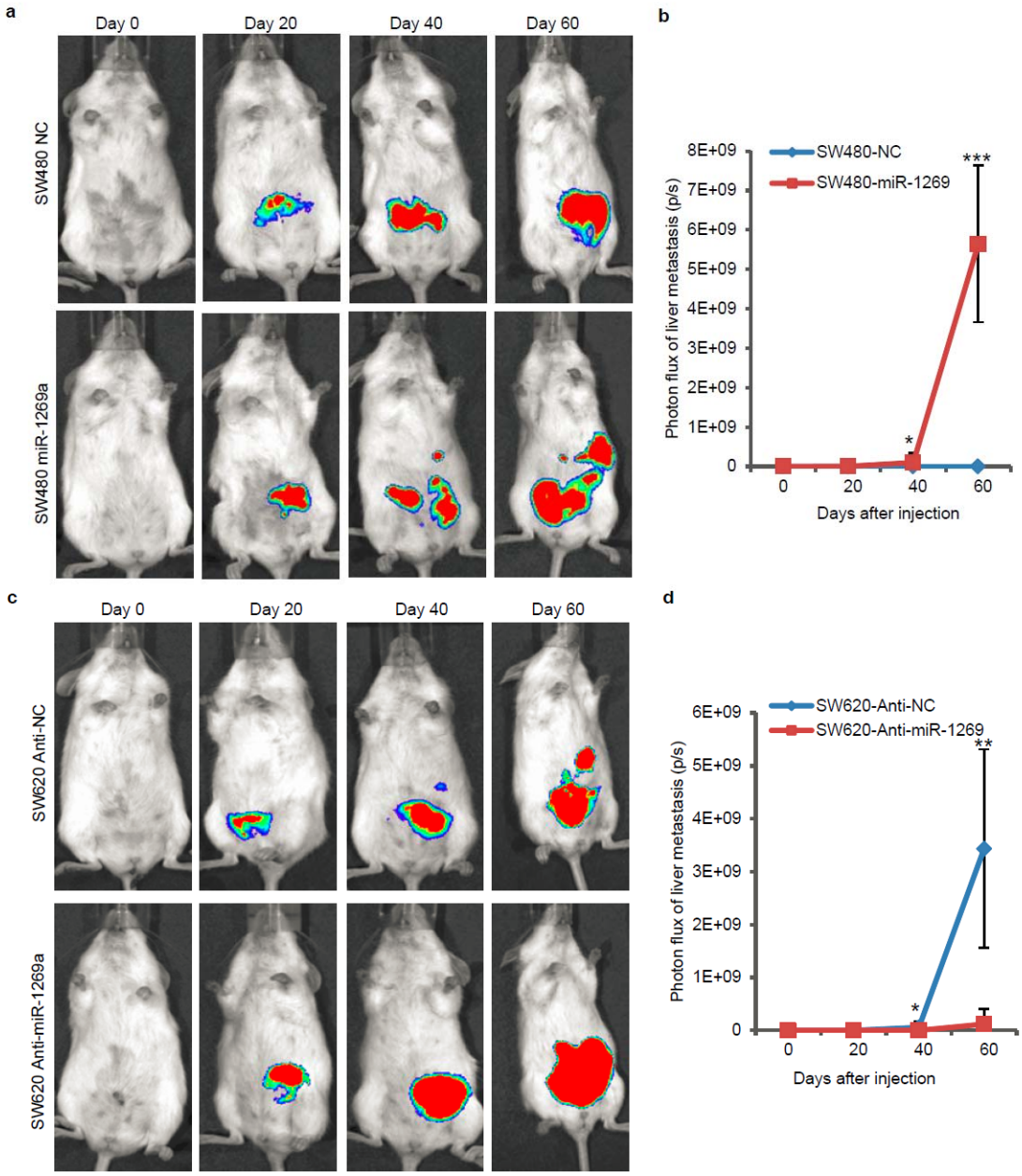

Supplementary Figure 4. miR-1269a promoted hepatic metastasis.
(**a**) Representative IVIS luciferase images taken from day 0 to day 60 post cecal implantation of SW480 cells. (**b**) Quantification of luciferase signals from hepatic metastases. (**c**) Representative IVIS luciferase images taken from day 0 to day 60 post cecal implantation of SW620 cells. (**d**) Quantification of luciferase signals from hepatic metastases. Error bars denote s.d. of 8 mice in each group. *, $p<0.05$; **, $p<0.01$, ***, $p<0.001$, Student's *t*-test.

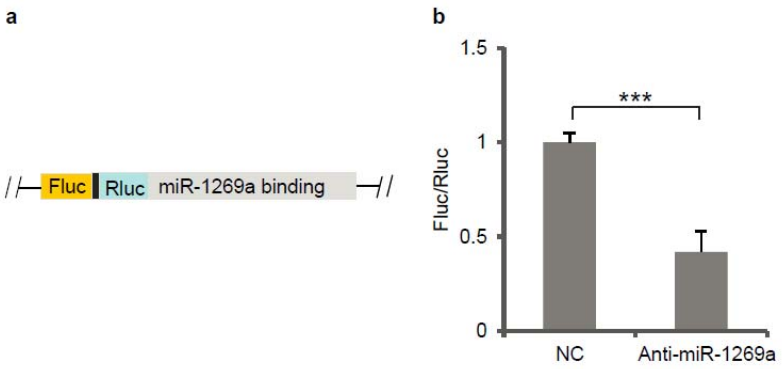

Supplementary Figure 5. shRNA silencing of miR-1269a.

(**a**) Schematic illustration of the reporter vector used in (b). miR-1269a binding sequences were cloned into the 3`UTR of Renilla luciferase (Rluc), with Firefly luciferase (Fluc) as a normalization control. Low miR-1269 expression leads to low Fluc/Rluc. (**b**) Luciferase reporter assay showing the knockdown efficiency of an anti-miR-1269a construct in SW620 cells. Error bars denote s.d. of triplicates. ***, $p<0.001$, Student's *t*-test.

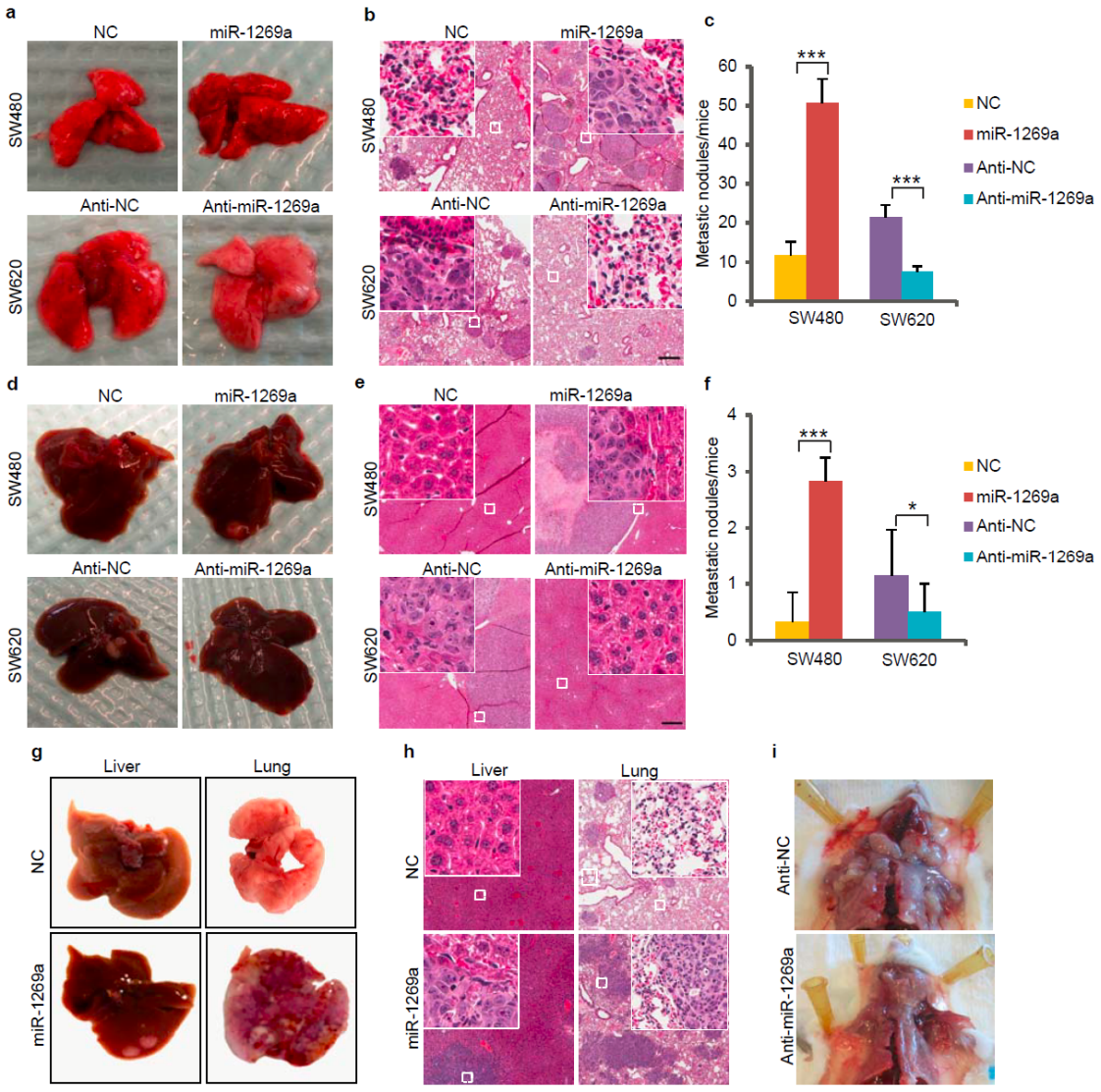

Supplementary Figure 6. miR-1269a promotes CRC cell colonization of liver and lung after intravenous injection.

(**a**-**c**) Representative images (a), H&E staining (b), and number of metastatic nodules (c) of lung metastasis. Ectopic miR-1269 expression promoted lung metastasis of SW480 cells (upper panel). Knockdown of endogenous miR-1269 by antisense RNA suppressed lung metastasis of SW620 cells (lower panel). (**d**-**f**) Representative images (d), H&E staining (e), and number of metastatic nodules (f) of liver metastasis. Ectopic miR-1269 expression promoted liver metastasis of SW480 cells (upper panel). Knockdown of endogenous miR-1269 by antisense RNA suppressed liver metastasis of SW620 cells (lower panel). (**g**-**h**) Representative images (g), H&E staining of liver and lung metastasis. Ectopic miR-1269 expression in HCT116 cells enhanced their liver and lung metastasis. (**i**) Representative images showing miR-1269 knockdown in LS174T cells reduced lymph node metastasis. In the H&E staining, inserts highlights big magnification of the indicated regions. Error bars denote s.d. of triplicates. *, $p<0.05$; ***, $p<0.001$, Student's *t*-test.

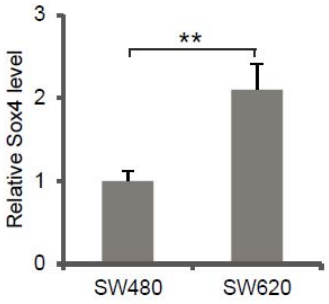

Supplementary Figure 7. Sox4 expression in SW480 and SW620 cells.
Sox4 expression levels in SW620 and SW480 cells, measured by RT-qPCR. Error bars denote s.d. of triplicates. **, $p<0.01$, Student`s *t*-test.

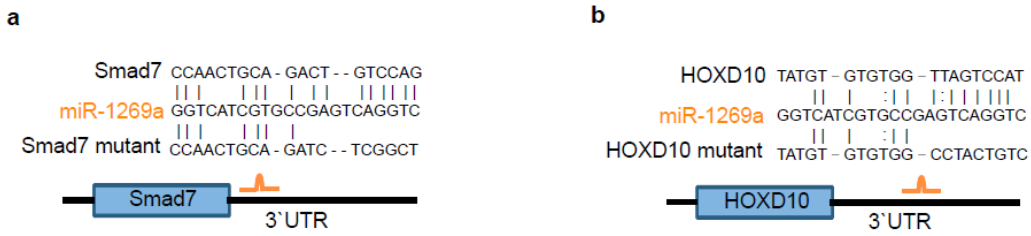

Supplementary Figure 8. Schematic representation of miR-1269a binding sites in the Smad7 and HOXD10 3`UTR.

(**a**) The predicted duplex formations between Smad7 3` UTR and miR-1269a, and mutation introduced to the seed region. (**b**) The predicted duplex formations between HOXD10 3` UTR and miR-1269a, and mutation introduced to the seed region.

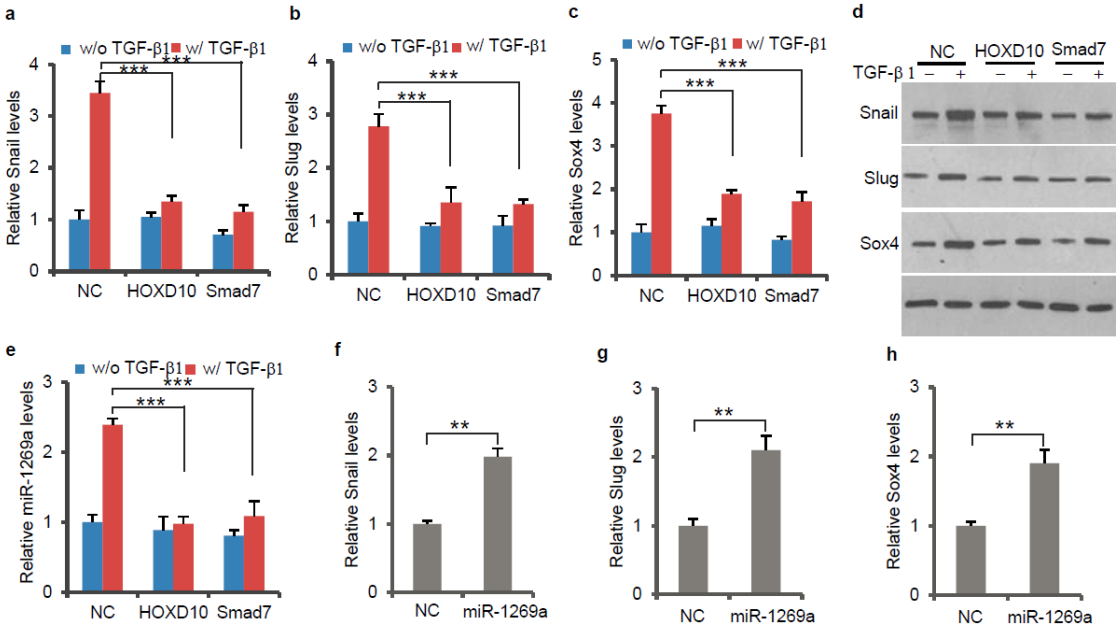

Supplementary Figure 9. miR-1269a upregulates TGF-β1 signaling by targeting Smad7 and HOXD10.

(**a-d**) RT-qPCR (a-c) and Western blot (d) showing ectopic expression of HOXD10 or Smad7 reduced TGF-b1 induction of Snail (a), Slug (b) and Sox4 (c) expression HT29 cells. (**e**) RT-qPCR showing ectopic expression of HOXD10 or Smad7 reduced TGF-b1 induction of miR-1269a in HT-29 cells. (**f-h**) RT-qPCR showing ectopic expression of miR-1269a upregulated Snail (f), Slug (g), and Sox4 (h) in HT29 cells. Error bars denote the s.d. of triplicates. **, $p<0.01$; ***, $p<0.001$, Student's *t*-test.

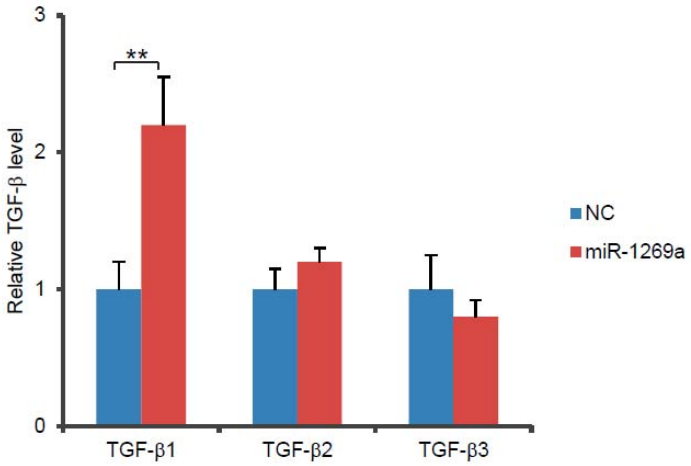

Supplementary Figure 10. The effect of miR-1269a on TGF-β expression.
RT-qPCR showing that ectoptic expression of miR-1269a increased TGF-β1 expression with little effect on TGF-β2 and TGF-β3 expression. Error bars denote the s.d. of triplicates. **, $p<0.01$, Student's *t*-test.

Fig.3

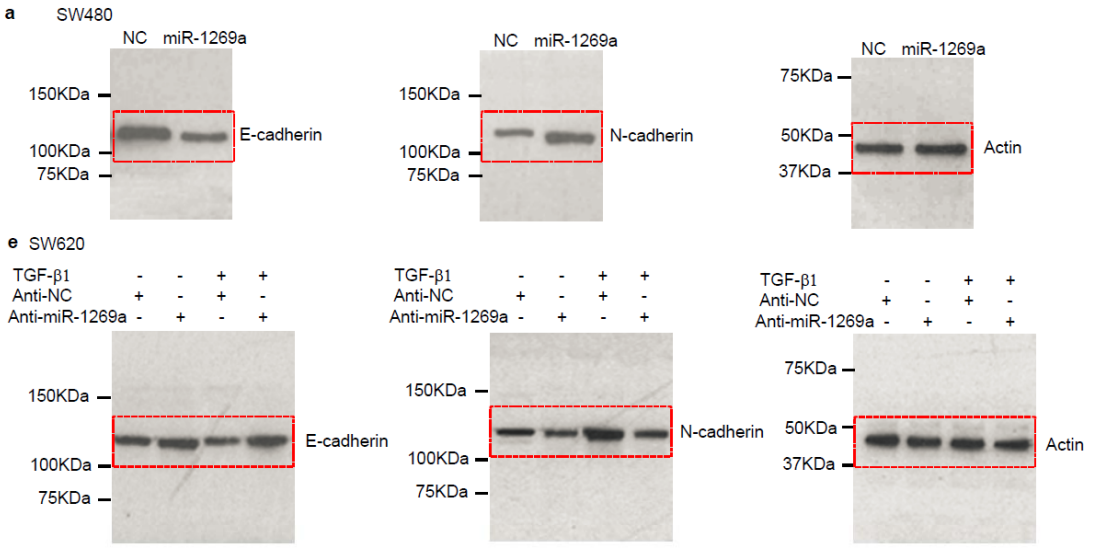

Fig.5

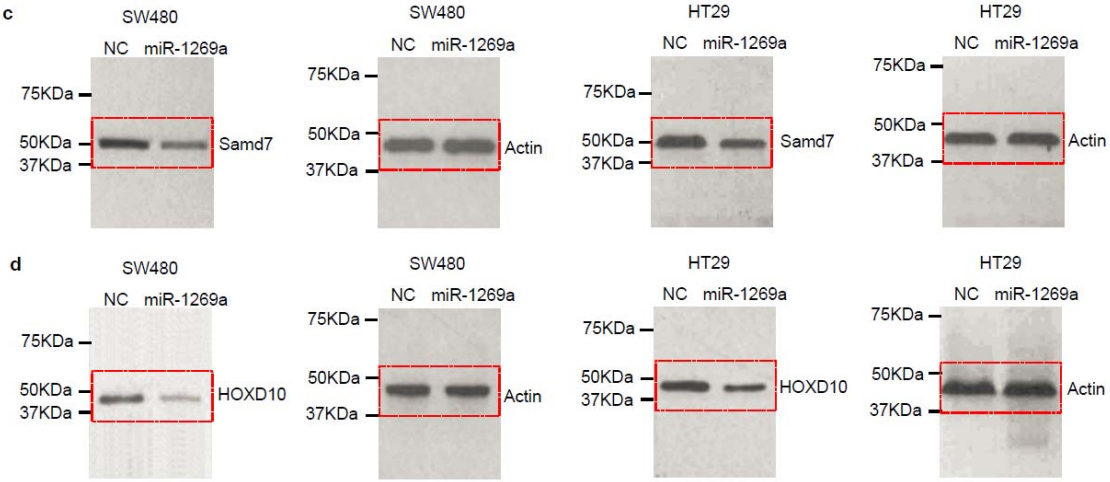

Supplementary Figure 11. Full scans of Western blots in Fig.3 and Fig.5.

Fig.6

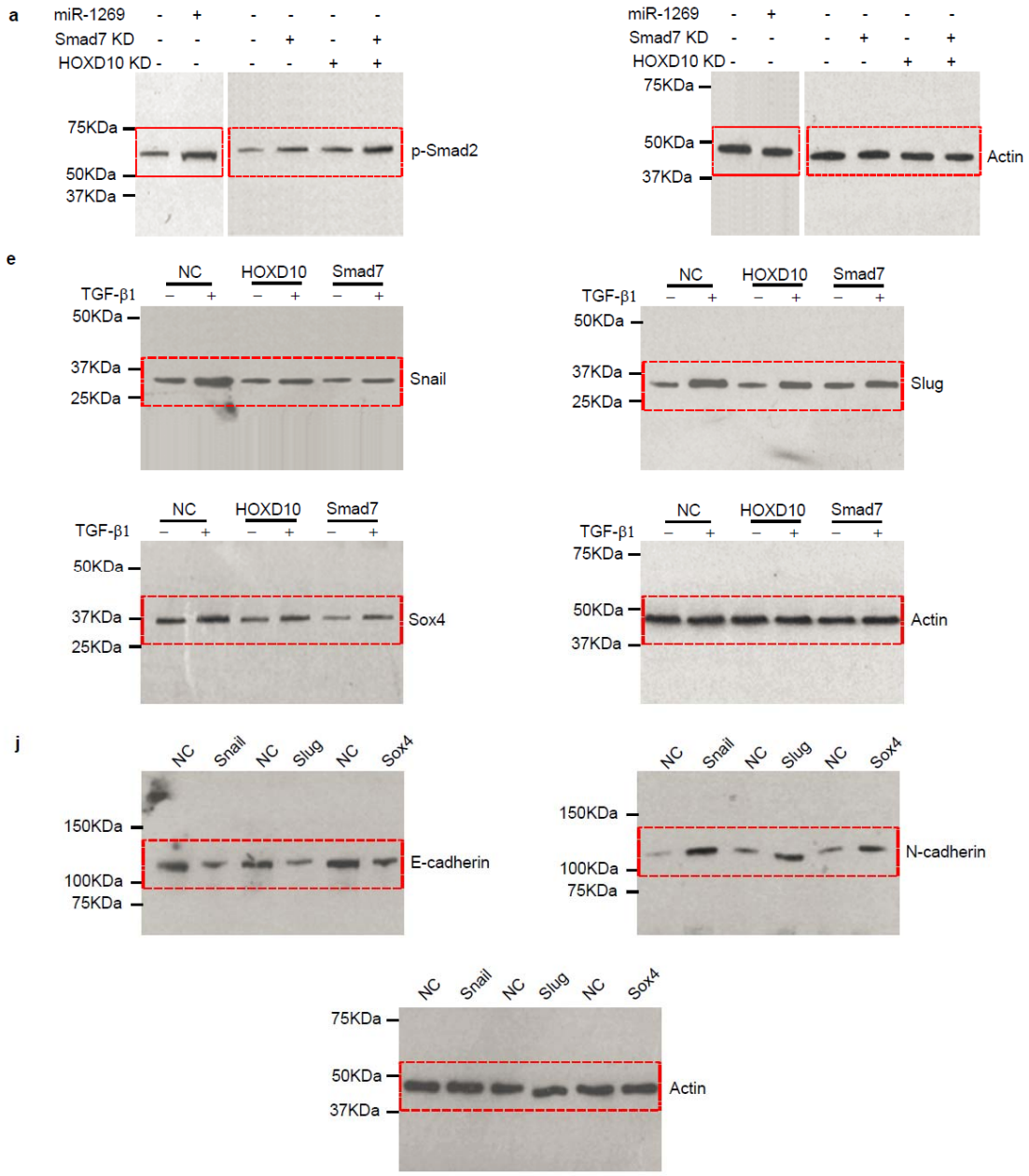

Supplementary Figure 12. Full scans of Western blots in Fig.6

Supplementary Table 1. Top 16 microRNAs upregulated in stage IV CRCs vs. stage I/II CRCs

Rank	MicroRNA	Means of read counts	Fold change	p value
1	hsa-mir-1269	240.56	2.74	1.12E-02
2	hsa-mir-105-1	15.60	2.69	2.89E-02
3	hsa-mir-105-2	16.10	2.63	3.53E-02
4	hsa-mir-34c	10.23	1.75	2.13E-05
5	hsa-mir-149	33.99	1.65	2.83E-06
6	hsa-mir-31	67.06	1.51	4.88E-02
7	hsa-mir-337	72.28	1.27	1.25E-02
8	hsa-mir-9-1	530.79	1.25	3.34E-02
9	hsa-mir-9-2	529.92	1.23	3.68E-02
10	hsa-mir-495	17.81	1.20	2.29E-02
11	hsa-mir-654	77.74	1.19	4.56E-02
12	hsa-mir-154	19.61	1.18	1.76E-02
13	hsa-mir-136	105.70	1.16	5.30E-03
14	hsa-mir-708	165.49	1.14	3.98E-02
15	hsa-mir-323	11.29	1.11	1.25E-03
16	hsa-mir-431	29.40	1.10	2.67E-02

Supplementary Table 2. Information of patients who provided tissues samples for comparing miR-1269a expression levels in early- vs. late-stage CRC tumors.

Patient	Gender	Age at visit	Stage	Differentiation	Lymph nodes
P1	M	52**.56**	I	Well	N0
P2	M	70	I	Poor	N0
P3	M	54	I	Moderate	N0
P4	F	84	I	Moderate	N0
P5	F	65	I	Moderate	N0
P6	M	43	IIA	NA	N0
P7	F	59	IIB	Poor	N0
P8	M	87	IIB	NA	N0
P9	F	62	IIB	Well	N0
P10	F	44	I	Moderate	N0
P11	M	85	I	NA	N0
P12	F	81	IIA	Moderate	N0
P13	F	74	IIIA	Poor	N1
P14	M	73	IIIA	Well	N1
P15	F	55	IIIA	NA	N1
P16	M	77	IIIC	Poor	N2
P17	F	68	IV	Poor	N2
P18	M	56	IV	Poor	N2
P19	F	21	IV	Moderate	N1
P20	F	46	IV	NA	N1
P21	F	73	IV	Moderate	N1
P22	M	66	IV	Poor	N1
P23	M	88	IV	Poor	N2
P24	F	73	IV	Poor	N1
P25	F	71	IIIC	NA	N2
P26	F	50	IIIC	Poor	N2
P27	F	39	IIIA	NA	N1
P28	M	37	IV	Poor	N2
P29	F	74	IIIC	Poor	N1

Supplementary Table 3. Computationally predicted miR-1269a target genes.

Refseq	Symbol	Description
NM_000020	ACVRL1	activin A receptor type II-like 1
NM_000033	ABCD1	ATP-binding cassette, sub-family D (ALD), member 1
NM_000046	ARSB	arylsulfatase B
NM_000073	CD3G	CD3g molecule, gamma (CD3-TCR complex)
NM_000080	CHRNE	cholinergic receptor, nicotinic, epsilon
NM_000084	CLCN5	chloride channel 5 (nephrolithiasis 2, X-linked, Dent disease)
NM_000125	ESR1	estrogen receptor 1
NM_000138	FBN1	fibrillin 1
NM_000020	ACVRL1	activin A receptor type II-like 1
NM_000033	ABCD1	ATP-binding cassette, sub-family D (ALD), member 1
NM_000046	ARSB	arylsulfatase B
NM_000073	CD3G	CD3g molecule, gamma (CD3-TCR complex)
NM_000080	CHRNE	cholinergic receptor, nicotinic, epsilon
NM_000084	CLCN5	chloride channel 5 (nephrolithiasis 2, X-linked, Dent disease)
NM_000125	ESR1	estrogen receptor 1
NM_000208	INSR	insulin receptor
NM_000212	ITGB3	integrin, beta 3 (platelet glycoprotein IIIa, antigen CD61)
NM_000217	KCNA1	potassium voltage-gated channel, shaker-related subfamily, member 1 (episodic ataxia with myokymia)
NM_002148	HOXD10	homeobox D10
NM_005904	SMAD7	SMAD family member 7